J Ther Eng, Vol. 11, No. 5, pp. 1−13, September, 2025

Journal of Thermal Engineering
Web page info: https://jten.yildiz.edu.tr
DOI: 10.14744/thermal.0000000

Research Article

# Effect of bristled shark scale structures on the aerodynamic characteristics of leading-edge protuberanced wing section

**S. SMRITHIKA[1], S. ARUNVINTHAN[1,*]**

[1]*Department of Aerospace Engineering, SASTRA Deemed University, Thanjavur, Tamil Nadu, 613401, India*

## ARTICLE INFO

*Article history*
Received: 28 May 2017
Accepted: 08 August 2017

**Keywords:**
Aerodynamic Force Coefficients; Biomimetics; Flow Control Leading-Edge Protuberances, Time-Series Data, Wind Tunnel Testing, Surface Pressure Distribution

## ABSTRACT

The present paper focuses its attention on assessing the influence of bristled shark scale structures over biologically inspired leading-edge protuberanced (LEP) airfoil section. It is worth noting that utilization of bristled shark scale structures as an effective flow control method remains untouched to date and this paper aims to study the same. NACA 63(4)-021 airfoil has been utilized as the baseline model in this study as it is closely reminiscent of the flippers of the Humpback whales. The test models include a baseline LEP model and two modified models M1 and M2 fitted with a single strip of shark scale structures at 0.6C and consecutive strips placed between 0.6 and 0.8C respectively. All the sets of experiments were conducted in the low-speed subsonic wind tunnel facility. The leading edge protuberanced wing utilized in the present study features an amplitude of 0.12C and wavelength of 0.5C based on the foundation developed by the previous researchers. The bristled shark scale structures inspired by the short-fin mako as well as the test model were 3D printed using PLA material at a resolution of 100$\mu/m$. The test models were experimentally evaluated for a wide range of angles of attack ranging from $0° \leq \alpha \leq 70°$ in increments of 5° at $Re$=1.71x10$^5$. Surface pressure measurements were obtained over the test models with the help of MPS4264 Scanivalve pressure scanner which are pneumatically connected to the pressure tapings. Aerodynamic forces and force coefficients were then estimated using pressure integration technique from the surface pressure measurements. Results reveal that the bristled shark scale tends to improve the aerodynamic characteristics in terms of lift increment and delay in flow separation. In other words, the modified models are effective as flow control means over the leading-edge protuberanced airfoil section. M1 and M2 improve the lift coefficient by 44% and 18.6% respectively when compared against the LEP baseline model. The prevailing spanwise gradient in the LEP baseline model is reduced around 85% in the modified model M1.

**Cite this article as:** Smrithika S, Arunvinthan S. Effect of bristled shark scale structures on the aerodynamic characteristics of leading-edge protuberanced wing section. J Ther Eng 2025;11(5):1−13.

***Corresponding author.**
*E-mail address: smrithika613@gmail.com, sarunvinthan@gmail.com

*This paper was recommended for publication in revised form by Editor-in-Chief Ahmet Selim Dalkilic*

## INTRODUCTION

One classical problem associated with the airfoils is the flow separation. The flow separation is a phenomenon involving separation of the boundary layer from the airfoil surface. Since, airfoils are widely utilized in various man-made applications like wind turbine blades, missiles, etc. [1-7], it is essential to control the flow separation over the airfoils. This necessitates flow control methods which can effectively delay the flow separation. Flow control methodologies are very much crucial in tailoring the aerodynamic characteristics of airfoil. These techniques manipulate the airflow over the airfoil which enhances lift, reduces drag, delays flow separation and hence improves the overall efficiency. Generally, flow control methods are classified into active, passive and hybrid. In the recent years, the use of biomimetics in flow control techniques piqued interest among the researchers. One such fascinating biomimetic study based on the shark scale denticular structure is presented in this research paper. Studies suggest that the shark scale denticular morphology could act like a vortex generator [8]. Originally, the shark skin has dermal denticles (scales) that impede body separation by providing local flow separation control, thus helping the shark to swim faster in water with least drag which inspired the aerodynamic designers and wind engineers. Arunvinthan et al. [8] replicated shark scale structures inspired by short fin mako as vortex generators and reported that the Shark scale-based vortex generators have improved the lift coefficient of an airfoil by 3.8% and delays the stall by controlling the flow separation thus reducing the drag. Vortex generators are small aerodynamic devices that are designed to improve the flow characteristics by delaying boundary layer separation and enhancing mixing between different layers of airflow.

Experiments carried out by researchers [9] confirmed the improvements in lift-to-drag ratio of denticle-inspired surfaces when compared with best-reported traditional low-profile vortex generators. Lang et al. [10] claimed that these shark scale structures behave in a similar fashion to streamwise riblets thereby reducing turbulent skin friction drag by 9.9%. Later, it was discovered that the shark's bristling denticles function as a vortex generator, a passive flow control device. According to the previous research [11], the results revealed that cavities developed in between the denticles, producing embedded vortices that are in opposition to wake creation. Lang et al. evaluated a simplified 3D shark scale based embedded cavity model with a flat base featuring 90° angle. Research results revealed that such square cavity formed by the bristled shark skin could effectively creates an interconnecting web of vorticity thus, rendering hydrodynamic benefit. This clearly shows that the bristled shark scale structure could potentially benefit as a flow control device. To gain more insight into the underlying flow physics, subsequently, Santos et al. [12] experimentally investigated the effectiveness of bristled shark skin as an effective means for boundary layer flow control. Results revealed that the angled shark scale structure tends to create a rotational flow near the wall thus injecting momentum into the boundary layer thereby converts the adverse pressure gradient into a favourable one, thus prolonging the flow attachment over the surface. Subsequently several researchers like Natarajan et al. [13] focused their attention on analyzing the hydrodynamic characteristics of such shark scale-based vortex generators and reported that the shark scale-based structures not only help in reattaching flow but also helps reducing the overall drag. These studies confirm the hydrodynamic benefits of the shark scale structure as a viable passive flow control technique. However, the difficulty and the challenge lies in replicating them to real-world scenarios. Researchers adopted several fabrication methods [14] such as Bio-replicated forming method, Direct manufacturing method, Indirect manufacturing method etc. to mimic the shark scale structures. Bio-replicated forming methods involve micro-embossing [15], vacuum casting [16], elastomeric stamping, etc. The Micro-embossing technique involves pressing a patterned mould into the substrate under controlled heat and pressure. The vacuum casting method utilizes a mould kept in a vacuum chamber. The resin is filled under the vacuum condition which eliminates the air bubbles. Even though these methods are simple to process they are limited to biological resources. Hence these methods cannot be used for wind tunnel testing. Direct manufacturing method for surface microstructures like surface machining (Walsh & Lindemann, 1984) [17] or surface-scratching are relatively easy to process but the processing efficiency is poor. Additionally, to achieve the similar sizing as the real-world short fin Mako played a significant challenge with the Direct Manufacturing methods as it is complicated, time-consuming, and costly. Indirect method can be classified into photolithography [18], laser etching [19], 3D-printing [20]. Photolithography technique utilizes light to transfer the pattern onto a light-sensitive layer on the substrate. After which material is added or removed based on the pattern. Direct manufacturing methods have high efficiency in the processing but the processing involved is complex. Considering all these issues and challenges with the various manufacturing methods, it has been decided to 3D print shark scale structures to create an economically feasible way while producing similar accuracy.

Recently, researchers have started experimenting with shark scale structures as a viable alternative for passive flow control means because of its intrinsic working nature. However, it should be noted that most of the research were aimed at investigating the hydrodynamic characteristics and hence the aerodynamic influence remains still lack. Considering the Reynolds number similarity, it is obvious that the shark-scale structures if implemented on airfoil will tend to behave in a similar fashion rendering aerodynamic benefit. Therefore, in the present study, the

authors planned to investigate the aerodynamic characteristics of such bristled shark scale structure. In the recent years, novel biomimetic Leading-Edge Protuberanced (LEP) wing section spurred research interest among many researchers because of its aerodynamic robustness. Therefore, it has been decided to test the influence of bristled shark scale structure on the aerodynamic characteristics of LEP wing. Frank E. Fish [21] initiated the study on the LEP wing inspired from the Humpback whales. Fish morphologically investigated the flippers of the humpback whales and reported that the biologically inspired LEP based wind turbine blades possess 25% more airflow than the conventional blade. Subsequently, Fish and Watts [22] acquired a patent for this technology. Miklosovic et al. [23] experimentally evaluated flippers with and without LEP and reported that LEP model offers stall delay benefit. Several researchers studied on the effectiveness of LEP in terms of amplitude [24], [25], wavelength [26], [27] and incidence angle [28] and reported that modifying the wavelength of LEP has negligible effects on the performance, while change in amplitude and incidence angle poses significant effects on the performance. Hansen et al. [29,30] investigated the working mechanism of the LEP and reported that the LEP generate vortices which change in direction of rotation with the change in the leading-edge geometry cancelling out each other resulting in a shorter wake creating no additional drag penalty. [31] proposed a different theory and suggested the local variation in the chord along the peak and the trough section of the LEP along with 3d spanwise flow results in non-uniform separation characteristics. Therefore, it provides extended flow reattachment even at greater angles thus providing aerodynamic robustness.

The present paper bridges both biomimetic studies of shark scale structures and humpback whale flippers. The primary objective of this study is to assess the aerodynamic performance characteristics of biologically inspired bristled shark scale structures on the novel LEP airfoil section. Therefore, in this present study, the influence of bristled shark scale structure as an effective means of flow control technique on the aerodynamic characteristics on the LEP wing was experimentally evaluated at $Re$=1.71x10$^5$. While most of the previous literatures refers to the investigation of shark scale structures on hydrodynamics, the present paper aims at exploring the influence of such shark scale structures on the LEP airfoil as an aerodynamic flow control technique. To the extent of authors knowledge, this will be the first of its kind in the world exploring the effect of bristled shark scale structures on the aerodynamic characteristics of bio-inspired LEP airfoil section. Surface pressure distribution were examined to gain more insight into the underlying flow physics. It is believed that the present study will act as a pilot study in utilizing shark scale structures as a passive flow control device for airfoils and its real-world applications.

**Table 1.** Comparison of literature with the experimental findings

| Author | Experimental / Numerical | Findings from the literature review | Relation with the Experimental findings |
|---|---|---|---|
| Arunvinthan et al. [8] | Experiment | Shark scale structures without bristling angle improve the lift coefficient of conventional airfoil by 3.8%. | The bristled shark scale structures improve the lift coefficient of LEP airfoil maximum by 44%. |
| Domel et al. [9] | Experiment | Shark denticles significantly improves the aerodynamics of conventional airfoils by extended flow attachment region thus enhancing lift with maximum of 323%. | The bristled shark scales enhance the aerodynamics of LEP airfoils by prolonged attachment of the flow (similar to conventional airfoils tested by Domel et al.). |
| Lang et al. [10,11] | Experiment | Bristled shark skin geometry effectively controls the flow separation and can be utilized as separation control mechanism. | Bristled shark scales extend the flow separation over the peak and trough section of the LEP airfoils which is evident from the CP vs x/C plots. |
| Santos et al. [12] | Experiment | Bristled shark skin control flow separation by eliminating adverse pressure gradient | Adverse pressure gradient formed at the peak section of LEP airfoil has been delayed by the incorporation of bristled shark scales. Therefore, bristled shark scale structures also delay adverse pressure gradient in LEP airfoils. |
| Natarajan et al. [13]; Wen et al. [20] | Experiment | Shark skin models were 3D printed using PLA material. | LEP airfoil section and bristled shark scale structures were 3D printed using PLA material. |

## MATERIALS AND METHODS

Experimental evaluations were performed to identify the effect of bristled shark scale structure affixed to biologically inspired LEP wing section at $Re$=1.71x10$^5$. All the test cases were tested in the low-speed subsonic open-circuit wind tunnel facility available at SASTRA Deemed University. The cross-section of the rectangular test-section is 300x300x1500 mm. The tunnel is activated by a fan powered by a 10HP motor and is capable of attaining a maximum speed of 60 m/s. The free-stream turbulence intensity at the test-section of the wind tunnel is 0.51%. A schematic representation of the wind tunnel with necessary equipment is shown in the Figure 1. NACA 63(4)-021 airfoil has been considered as the baseline airfoil profile in this study. The airfoil selection is based on the previous literatures. Several researchers have reported that NACA 63(4)-021 airfoil strongly reminiscent the cross-section of the flippers of humpback whale and hence NACA 63(4)-021 airfoil was chosen as the baseline airfoil profile. NACA 63(4)-021 airfoil is a member of 6-series airfoils and is symmetrical in nature. The detailed nomenclature based on the 6-series airfoil is as follows:

First digit "6" indicates the airfoil is from the 6-series. Second digit "3" describes the chordwise location of minimum pressure on the airfoil at the designed lift coefficient (Cl). This digit specifies that the minimum pressure is at 30% of the chord from the leading edge. Third digit "(4)" refers to the range of lift coefficient in which the favourable pressure gradient exists on both surfaces. Fourth digit "0" represents the design lift coefficient in tenths. Last two digits "21" represents the maximum thickness of the airfoil as a percentage of the chord length. In this case, the maximum thickness is 21% of the chord length.

Aiming at incorporating protuberances at the leading-edge, the sinusoidal protuberances of the baseline model was greatly influenced by two parameters namely amplitude (A) and wavelength (λ) were utilized as outlined in previous literatures [28], [32]. Since the present study focuses its attention to assess the effect of bristled shark scale on the LEP wing, the parameters A and λ of the sinusoidal LEP has been kept constant as 0.12C and 0.5C respectively throughout this study. The test model considered in this study has a mean chord length of chord length of 100 mm and span 300 mm the entire test-section thus making it as an infinite model. The baseline LEP model was then fabricated using Polylactic acid (PLA) material via 3D printing at a resolution of 100μ. Since the test model possess a varying chord, the surface pressure was measured at two different locations namely peak (i.e., chord maxima) and the trough (i.e., chord minima). The surface pressure tapings were equi-distributed over the LEP wing. A total of 50 pressure taps were made over the airfoil surface. 20 pressure taps were equi-distributed over the peak region and 16 pressure taps over trough region while remaining taps were distributed along the span of the model. The spacing between each taping is 9mm and the diameter of each pressure tap is approximately 1 mm.

The fabrication of bristled shark scale involves 3D printing utilizing the same poly lactic acid material. The shark scale models featuring chord length of 10 mm and span 6 mm with leading-edge amplitude of 2 mm has a bristling angle of 20°. The shark scale model is resting in a pillar with a height of 5 mm as shown in Figure (c) & (d). This 3D printed bristled shark scale models were affixed to the baseline LEP wing at 60% of the mean chord length (hereafter named as M1). To gain some insights on the effect of shark scale structures on the flow over the LEP wing, the structures were also arranged continuously from 60% to

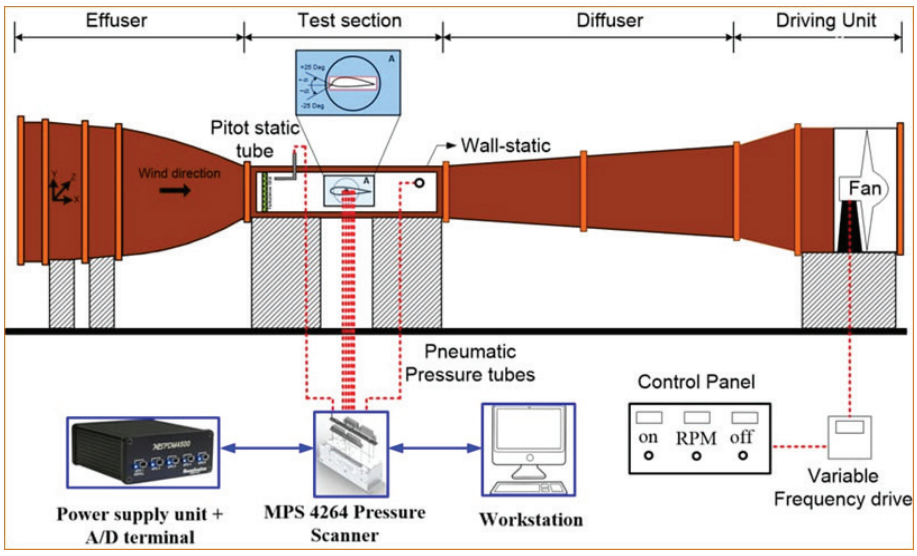


**Figure 1.** Schematic representation of wind tunnel setup.

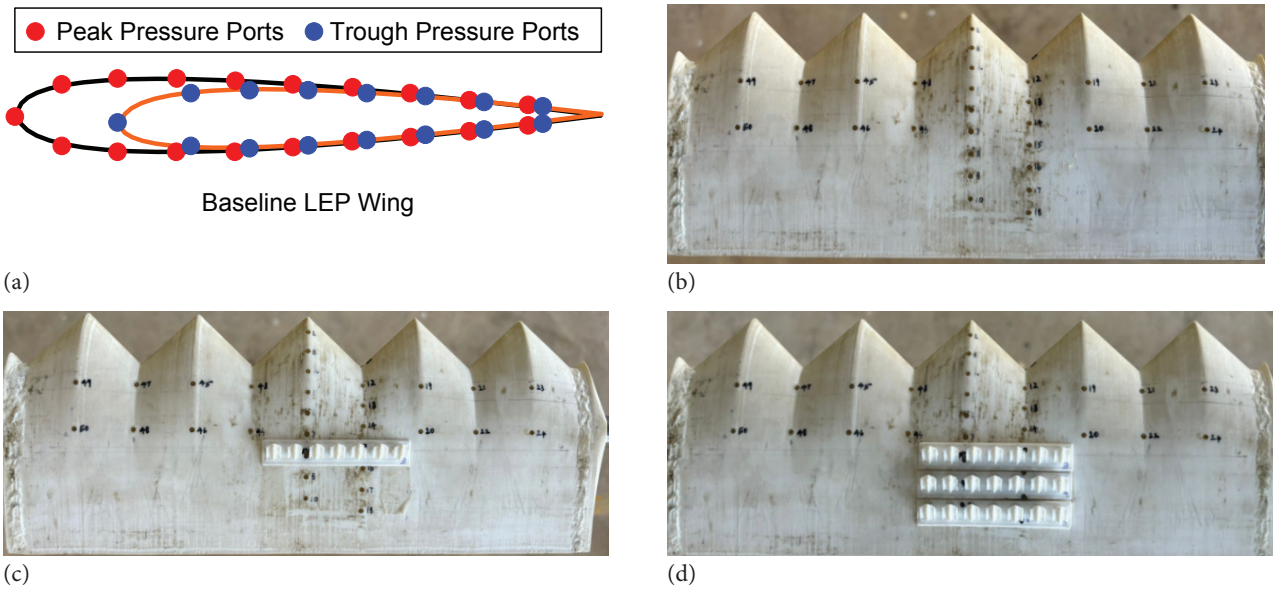


**Figure 2.** (a) Schematics of distribution of pressure ports (b) Real image of LEP baseline airfoil (c) Real image of modified M1 model (d) Real image of modified M2 model.

80% of the mean chord length of the LEP wing (hereafter named as M2). A visual representation is shown in the Figure 2. The surface pressure of the test models were then measured through the pressure taps which are pneumatically connected to simultaneous MPS4264 Scanivalve pressure scanner. The aerodynamic lift, drag forces and surface pressure distribution acting over the modified and unmodified equivalents were then estimated using pressure-integration technique [33-35] to yield lift, drag and pressure coefficients.

$$F_D = \sum(\Delta P) \times S_i \times cos(a + \frac{\pi}{180}\theta) \quad (1)$$

$$F_L = \sum(\Delta P) \times S_i \times sin(a + \frac{\pi}{180}\theta) \quad (2)$$

$$C_D = {}^{F_D}/_{0.5\rho v^2 s} \quad (3)$$

$$C_L = {}^{F_L}/_{0.5\rho v^2 s} \quad (4)$$

$$C_P = {}^{\Delta P}/_{0.5\rho v^2 s} \quad (5)$$

The uncertainties involved in the experiments like Buoyancy, solid blockage, wake blockage etc. and the instrumental uncertainties included in the present study along with their correction factors are tabulated as Table 2.

## RESULTS AND DISCUSSION

The shark scale models affixed to the clean baseline LEP wing was primarily evaluated to identify its influence on the flow characteristics and aerodynamic behaviour of the bio-inspired LEP wing section. The modified models (M1 and M2) were tested in the wind tunnel using surface pressure measurement at *Re*=1.71x10$^5$. The results obtained for the modified models were compared against the baseline LEP wing section as shown below. Figure 3 represents the variation of time-averaged coefficient of lift ($C_L$) vs the angle of attack (α) for all the test cases operating at *Re*=1.71x10$^5$. In the figure, square denotes the $C_L$ values for model M1, circle denotes the $C_L$ values for model M2 and star denotes the $C_L$ values for LEP Baseline model. It can be observed from the graph that the $C_L$ curve gradually increases in the direction of increasing angle of attack until $\alpha$ = 40°. For instance, it can be observed that the baseline LEP model exhibits a maximum lift coefficient ($C_{Lmax}$) of 0.84 at $\alpha$ = 40°. Beyond which with the further increase in the angle of attack, the lift coefficient gradually decreases. It can be easily seen from the figure that both the bristled shark scale models (M1 and M2) affixed to LEP wing exhibits significantly higher lift coefficient at all angles of attack than its unmodified equivalent. Therefore, it becomes clear that the presence of 3D printed shark scale over the LEP wing alters the flow characteristics by effectively inducing the momentum into the boundary layer and thus rendering aerodynamic benefits in terms of $C_L$ increment. For instance, M2 model exhibits the maximum lift coefficient ($C_L$) of 0.99 which is 17.8% higher than the baseline model. At the same $\alpha$ = 40°, the modified M1 model exhibits a maximum lift coefficient of about 1.05 representing lift

**Table 2.** Uncertainties and their correction factor

| Uncertainty | Correction method | Substitution | Correction factor |
|---|---|---|---|
| **Buoyancy correction** | Glauert method: $D_B = \frac{1}{2}\pi\lambda_2 t^2 P'$ | $\lambda_2 = 1.4$ [36] $t = 0.021\ m$ $P' = 0.01\ N/m^2$ | 0.00000969 |
| **Solid blockage correction** | Thom's method: $\varepsilon_{sb} = \frac{K_1(Model\ Volume)}{c^{3/2}}$ Model Volume = 0.7 × model thickness × model chord × model span; | $K1 = 0.74$ *Model Volume* = 0.000441 $c = 0.09$ | 0.0120 |
| **Wake blockage correction** | Allen and Vincentti method: $\Delta C_{d,wb} = \Lambda\sigma$ $\sigma = \left(\frac{\pi^2}{48}\right)\left(\frac{C}{h}\right)^2$ | $\Lambda = 0.36$ [36] $\sigma = 0.0616$ | 0.0221 |
| **Instrument and Data Error** | MPS4264 miniature Scanivalve pressure scanner – OEM error intimation | - | full-scale error of ±0.06% |

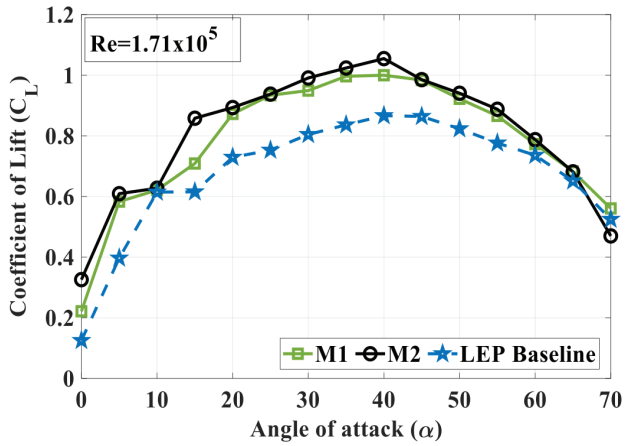


**Figure 3.** Aerodynamic lift coefficient ($C_L$) vs Angle of attack (α)

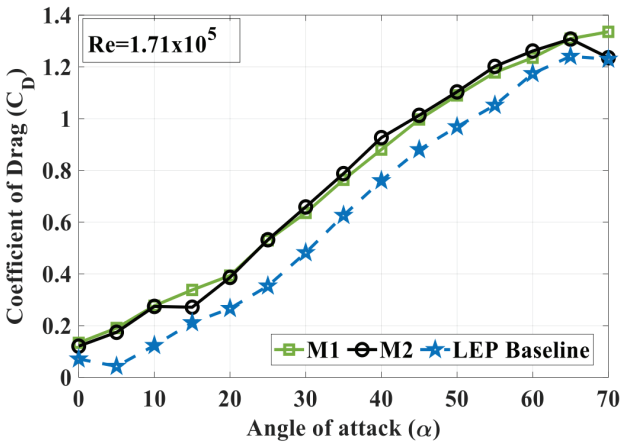


**Figure 4.** Aerodynamic drag coefficient ($C_D$) vs Angle of attack (α)

increment of 25% when compared against the LEP baseline model. The similar trendline can be observed in the pre-stall angles as well. For instance, at $\alpha$ = 15° the modified model M1 and M2 displays a $C_{Lmax}$ of 0.85 and 0.70 which is 44% and 18.6% higher than baseline LEP respectively. Based on the obtained experimental results, it can be summarized as the addition of shark scale structures over the LEP baseline can augment the lift characteristics of the LEP wing section.

Figure 4 shows the comparison of drag characteristics of the modified models with the unmodified equivalent for various α. In the figure, square denotes the $C_L$ values for model M1, circle denotes the $C_L$ values for model M2 and star denotes the $C_L$ values for LEP Baseline model. It is important to note here that the drag illustrated in this study corresponds to pressure drag alone and skin friction drag is not considered. It is notable from the figure that the baseline LEP exhibits the lowest drag than the modified models throughout all angles of attack. It could be understood that bristled shark scale structures induces turbulence creating perturbations in the flow thereby resulting in higher pressure drag. To gain more insights on the aerodynamic behaviour, surface pressure distribution were plotted against the chordwise position (x/C) for $\alpha$ = 5° as shown in the Figure 5, 6. As the test model is a non-constant chord model featuring varying chord length along the chord-maxima and the chord-minima section, it becomes important to investigate the pressure distribution over both the chord-maxima and chord-minima region as shown in Figure 5, 6.

The surface pressure distribution in terms of pressure coefficient ($C_P$) plotted against x/C for test models at α=5° as presented in Figure 5, 6. It becomes clear from the figure

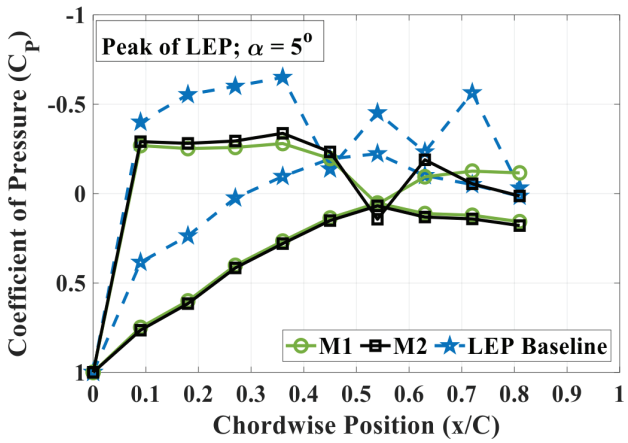


**Figure 5.** Surface pressure distribution along the chordwise position (x/C) for α = 5° (peak region)

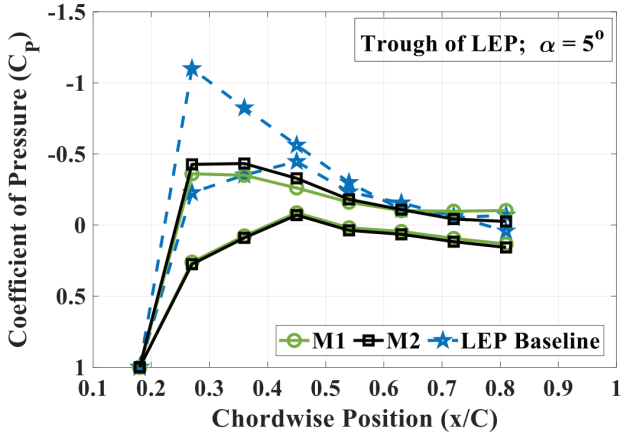


**Figure 6.** Surface pressure distribution along the chordwise position (x/C) for α = 5° (trough region)

that the flow over the trough region remains attached in comparison against the peak region. This is because of the increased flow velocity over the trough region. For instance, it is notable from the figure 6 that peak negative suction pressure is seen at the trough section indicating that the majority of the freestream flow goes behind the trough region. It is understandable that a strong acceleration occurs at trough region when compared against the peak region thereby creating a spanwise flow. Evidently, the suction pressure on the trough region is lesser than the peak region indicating the accelerated flow at trough section. For Instance, if the velocity behind the trough section is very high, then the pressure will be relatively low in comparison against the peak region. However, as its well known that, when the flow over the peak is relatively smaller than the trough section, the high-pressure region from the peak tends to move to the low-pressure suction region happening behind the trough section thereby leading to reenergize the trough flow sacrificing the peak flow. This spanwise flow induced by the change in the pressure over the peak and the trough section keeps the flow attached over the trough section of the LEP. In simpler words, it could be explained that the spanwise pressure gradient created between the peak and the trough section draws low-inertial boundary layer molecules from the peak. This could be observed from the Figure 5 that at around 0.4C for the peak section, an increase in the pressure can be seen. As it is known that the increase in the pressure signifies reduction in velocity, this can be attributed to the following explanation: as the low-inertial boundary layer molecules from the peak are drawn towards the trough region an increase in the pressure is felt over the peak region at 0.4C. Studies [37] suggest that when a low-inertial boundary layer molecules are transported away because of the spanwise pressure gradient, the flow will be replaced by a high-momentum fluid drawn from above fluid layers thereby reenergizing the flow. This in turn holds in good agreement with the surface pressure characteristics for the baseline LEP wing displayed in Figure 5 which indicates the flow reattachment signified by the decrease in pressure around 0.5C. Subsequently the flow undergoes similar phenomena at 0.7-0.8C as well. Therefore, based on these results, it can be claimed that the low-inertial boundary layer molecules driven from the peak section transported towards the trough section by the spanwise pressure gradient is held responsible for the intended aerodynamic benefit. In the case of the modified models affixed with shark scale structures, it is clearly evident that the peak negative suction pressure observed over both the peak and the trough section is significantly lesser when compared against the baseline LEP model. For instance, M1 model attains a peak negative pressure of -0.33 and -0.43 in the peak region and trough region respectively. It is speculated that the reduction in the flow acceleration over the upper surface of the modified LEP model is due to the presence of the shark scale structures. As it is well known that the pressure disturbances can propagate upstream in subsonic flow, the changes in the local pressure distribution induced by the shark scale structure influences the flow characteristics over the suction side of the airfoil. In other words, the reorganization of the flow upstream to accommodate the downstream disturbance induced by the shark scale structures results in the reduction of flow acceleration over the suction side of the airfoil signifying reduction in the peak negative suction pressure. Furthermore, it can be claimed that with the incorporation of shark scale structures the spanwise flow from peak to trough changes considerably. For instance, it could be seen that for the baseline LEP model, the peak negative suction pressure at the peak and the trough section corresponding to 0.1C is -0.40 and -1.09 whereas for the modified models M2 and M1, the peak negative suction pressure at 0.1C for the peak and the trough section reduces to -0.29 & -0.42 (for M2) and -0.26 and -0.36 (for M1) respectively. This clearly quantifies the reduction in the spanwise pressure gradient existing between the peak and the trough section for the modified models. In simple words, roughly 80% of the spanwise pressure gradient has reduced

with the introduction of the shark scale structures resulting in lesser suction at the trough region in comparison with the baseline LEP model. The reduction in the spanwise pressure prolongs the flow attachment regime over the peak section by limiting the transportation of the low-inertial boundary layer molecules from the peak section. However, as the name itself indicates "low-inertial boundary layer molecules" eventually they separate after a short while. Results indicate that following the peak negative suction pressure for the baseline LEP model at 0.1C, the $C_p$ increases with the increase in the chordwise position till 0.4C indicating the flow acceleration. Beyond 0.4C the pressure coefficient increases abruptly indicating the reduction in the flow velocity. It is speculated that this reduction in the flow velocity over the baseline LEP model is induced by the spanwise flow. However, in the case of the modified LEP models affixed with shark scale structures, as nearly 80% of the spanwise flow is diminished, the flow continues to attach till 0.5C for both the M1 and M2 models. Consequently, as the model M1 has even more reduction in the spanwise pressure gradient (approximately 85%) a similar pressure coefficient trendline can be observed but with more gradual slope (between 0.5-0.6C) in comparison against the M2. Therefore, it becomes clear that with the incorporation of shark scale structures on the LEP wing, the shark scale structure reorganizes the flow altering it favourably redistributing the majority of the spanwise pressure gradient in terms of prolonged flow attachment over peak section provides aerodynamic benefit. Furthermore, the alternate separation and reattachment pattern observed at the baseline LEP wing is stabilized with the introduction of shark scale structures as seen from the figure. It is believed that the small vortices induced by the shark scale structures mix higher-momentum fluid into the boundary layer thereby energizing the boundary layer, making it more resistant to separation. The delayed separation along with enhanced flow attachment observed over the modified models with shark scale structure increases the pressure gradient between the suction side and the pressure side of the model thereby resulting in higher lift coefficients in the modified model. It is of interest to note that out of the modified models M1(single-strip) and M2 (three-consecutive strips), M1 has the least drag profile. To further ascertain this behaviour, surface pressure contours were plotted for both the baseline and the modified M1 model is depicted in Figure 7-10.

It can be clearly seen from the figure that for the baseline LEP model, over the peak region (Fig. 7), followed by an initial increase in the pressure at the leading-edge signifying the stagnation point, with the acceleration in the flow, the pressure gradually decreases. But it could be observed at around 0.05m chordwise position, the pressure increases indicating the flow separation induced by the spanwise flow. Following which the flow reattaches and separates alternatively as

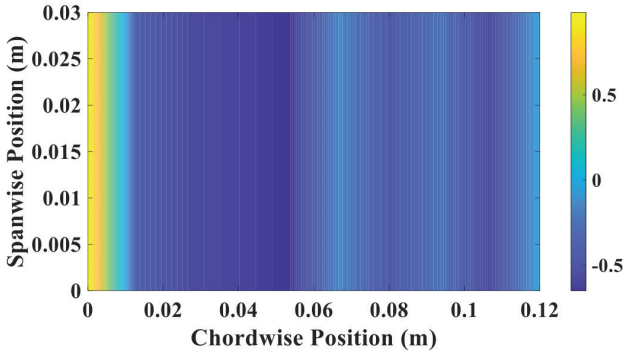


**Figure 7.** Surface pressure contour over LEP baseline peak at α=5°

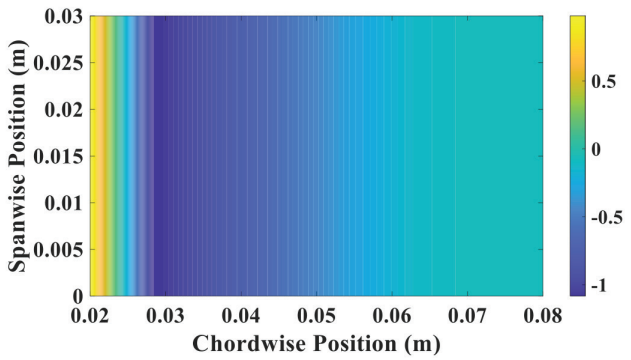


**Figure 8.** Surface pressure contour over LEP Baseline trough at α=5°

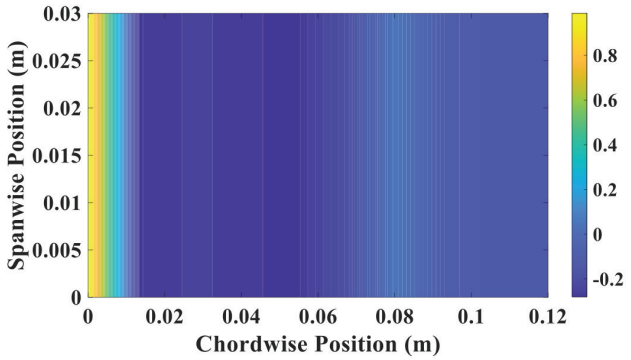


**Figure 9.** Surface pressure contour over M1 peak at α=5°

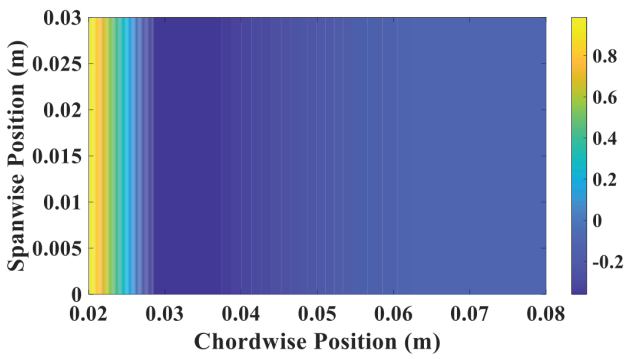


**Figure 10.** Surface pressure contour over M1 trough at α=5°

indicated in the Figure 6. On the other hand, the flow remains continuously attached over the suction side of the airfoil at the trough section as shown in Figure 8. Similarly, the peak and trough surface Pressure contours were plotted for the modified model with bristled shark scale structures (M1) in the Figure 9, 10. In the case of the M1 model, it is evident that the flow instability that previously occurred near the vicinity of the trailing edge in the LEP baseline model disappears completely. Furthermore, the non-uniform separation characteristics observed in the LEP baseline gets reorganized and redistributed with the incorporation of bristled shark scale structures. It should however be noted that the presence of the bristled shark scale structures in fact give a slight increase in the pressure ahead of the model. The reduction in the spanwise flow with the introduction of shark scale structures keeps the flow attached over both the peak and the

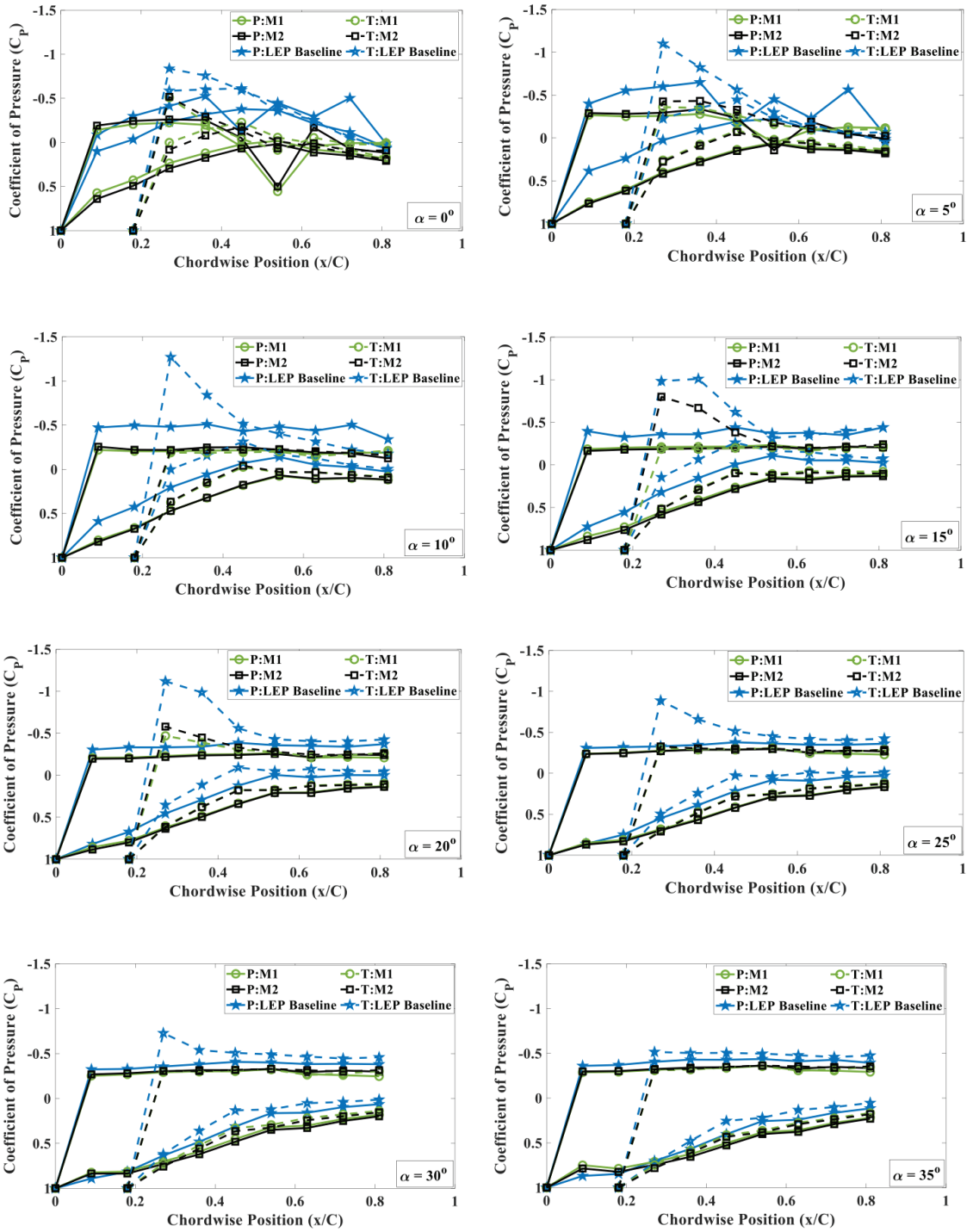

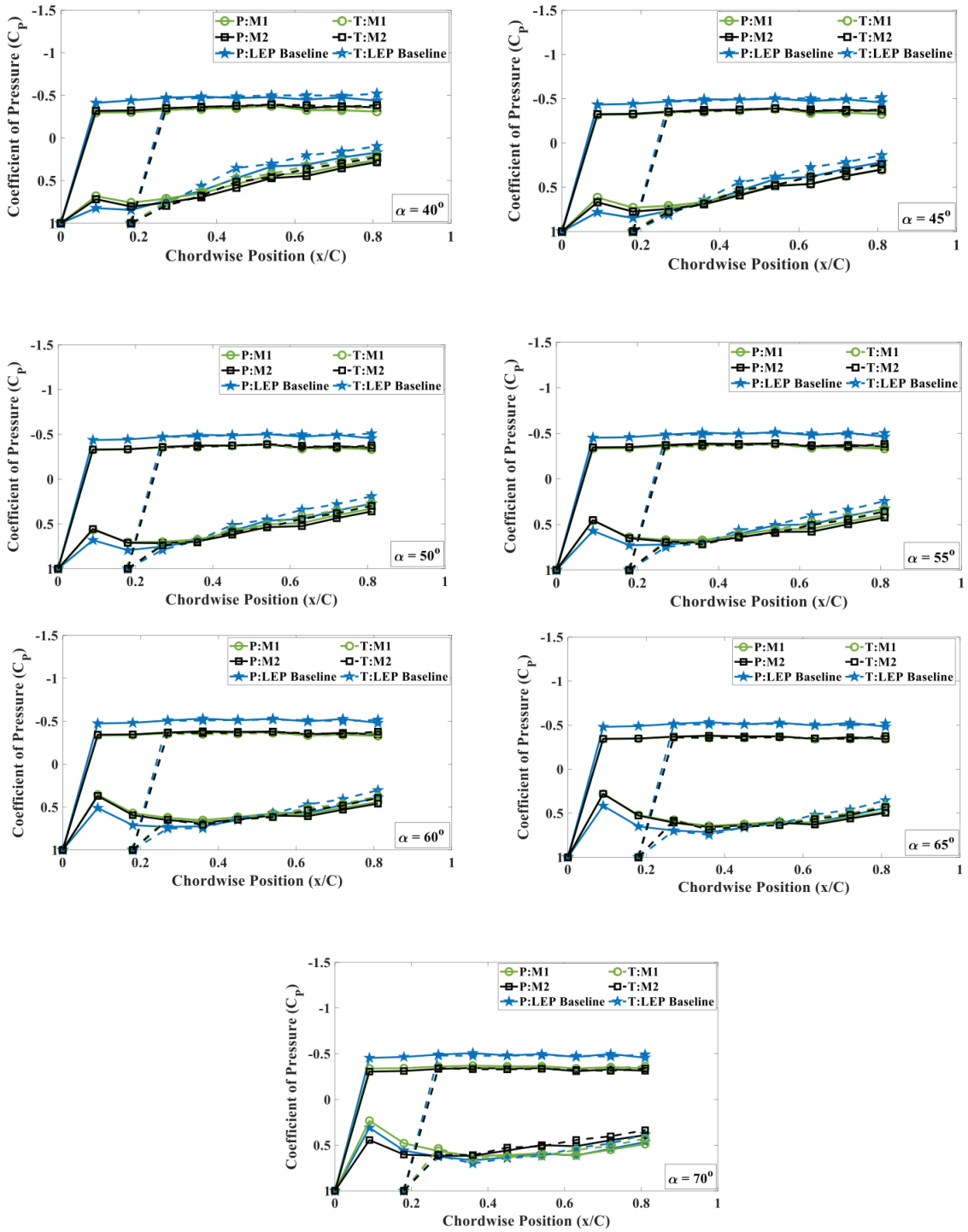


**Figure 11.** Surface pressure distribution along the chordwise position (x/C) from α= 0° to 70°

trough for a longer distance thereby providing delay in flow separation.

Figure 11 compares the pressure distribution over the baseline LEP and the modified models (M1 and M2) for various α from 0° to 70°. The solid green line indicates the pressure distribution over the peak section of M1 model, solid black line refers the pressure distribution over the peak section of M2 model while solid blue line for peak section of LEP baseline. Similarly, dashed line represents the pressure distribution over trough section of modified models and the LEP baseline model. Since LEP is a non-constant chord model, as discussed in the previous section, it could be seen that both the peak and the trough region experiences an altogether different flow pattern. Results reveal

that the extended flow attachment is seen over trough region rather than the peak section for the modified and LEP baseline models at lower α values. It is of interest to note that despite the addition of bristled shark scale structures on the modified model, the non-uniform separation characteristics prevalent over the baseline LEP wing could be still observed on the modified models. However, the addition of bristled shark scale structure influences the surface pressure characteristics, by energizing the boundary layer through the vortices produced by the shark scales. This in turn increases the net pressure gradient of the airfoil. At very larger values of α, the flow gets separated completely over both peak and trough section of the unmodified and modified equivalents. The graph plotted in the Fig. 11 reveals that the pressure gradient existing between the suction and the pressure side for the modified models (M1 and M2) is larger in comparison with the unmodified equivalent. The flow is attached over both peak and trough section of the bristled shark scale affixed models at $\alpha = 0°\&5°$. From $\alpha = 10°$ *to 2*0°, the flat section at the peak region depicts the separated flow whereas the trough section exhibits attached flow over the modified models as well as unmodified test case. The plateau region presented in the $C_P$ vs x/C plots indicate constant pressure region, which in other words can be expressed as the flow separation regime. Though, the flow has been separated, the pressure gradient for the modified models is higher when compared against the baseline LEP model, thereby resulting in higher lift coefficients. Overall, it can be concluded that the modified shark scale models effectively alters the flow characteristics providing delayed separation, enhanced flow attachment, stable flow structure in proximity with the trailing edge and thus, rendering aerodynamic benefits.

## CONCLUSION

The concluding remarks and findings are as follows:

- Bristled shark scale structured airfoil models exhibits enhanced lift characteristics at both the pre-stall and post-stall angles against its unmodified equivalent.
- At pre-stall angles ($\alpha = 15°$), the modified model M1 (single strip at 0.6C) exhibits a maximum lift increment of 44%, while M2 (Shark scale strips between 0.6-0.8C) shows a peak lift increment of 18.6% in comparison against the LEP baseline model.
- At post-stall angles ($\alpha = 40°$), M1 and M2 exhibits a maximum lift increment of 25% and 17.8% against the LEP baseline model.
- Surface pressure distribution over the test models with bristled shark scale structure clearly shows that the presence of shark scale structure effectively alters the flow characteristics.
- Results reveal that small vortices induced by the shark scale structures mix higher-momentum fluid into the boundary layer thereby energizing the boundary layer, making it more resistant to separation in addition to the 85% reduction in the span wise flow, makes the modified model outperform the baseline unmodified equivalent.

Experimental results proved that the bristled shark scale structures can effectively alter the aerodynamic characteristics and therefore can be used as a viable passive flow control device. One of the challenges involved in this present study is the dislodging of 3D printed bristled shark scale structures affixed to the LEP wing section at high Reynolds number. Therefore, in the future, instead of affixing 3D Printed shark scale structures they should be printed directly over the airfoil section itself. But it should be noted that this will increase the model count and cost incurred for the research with the testing of different patterns and sizes of bristled shark scale structures. Attempts to decode the underlying flow physics in detail should be entertained in the near future to potentially utilize this technology in real-world applications. Since the experimental evaluation of biomimetic LEP airfoil with shark scale structures yielded a voluminous amount of pressure data, statistical analyses like 0-1 test, recurrence quantification analysis (RQA) etc. will also be a potential future work.

## NOMENCLATURE

| | |
|---|---|
| LEP | Leading-edge protuberance |
| $\theta$ | Angle of incidence on the $i^{th}$ port (°) |
| $C_D$ | Coefficient of drag |
| VG | Vortex Generator |
| SSVG | Shark Scale Vortex Generator |
| SEM | Scanning Electron Microscopy |
| $\lambda$ | Wavelength (m) |
| $A$ | Amplitude (m) |
| $C$ | Chord length (m) |
| PLA | Polylactic acid |
| $v$ | Velocity (m/s) |
| M1 | Bristled shark scale at 60% of the mean chord length |
| $\lambda_2$ | body shape factor |
| $P'$ | slope of longitudinal static pressure gradient curve |
| $\Delta_{Cd,wb}$ | Wake blockage correction |
| $\Lambda$ | body shape factor |
| $h$ | Tunnel height (m) |
| $Si$ | Area ($m^2$) |
| $\alpha$ | Angle of attack (°) |
| $C_L$ | Coefficient of lift |
| $C_P$ | Coefficient of pressure |
| $x/C$ | Chordwise location |
| $Re$ | Reynolds Number |
| $\Delta P$ | Net Pressure (N) |
| $F_L$ | Lift force (N) |
| $F_D$ | Drag force (N) |
| $\rho$ | Density of the fluid ($kg/m^3$) |
| $s$ | Reference area ($m^2$) |
| M2 | Bristled shark scale at 60% to 80% of the mean chord length |

t body thickness (m)
$D_B$ Glauert's buoyancy correction factor
$c$ test-section area ($m^2$)
$K_1$ Constant value for wing spanning the tunnel breadth

## AUTHORSHIP CONTRIBUTIONS

Authors equally contributed to this work.

## DATA AVAILABILITY STATEMENT

The authors confirm that the data that supports the findings of this study are available within the article. Raw data that support the finding of this study are available from the corresponding author, upon reasonable request.

## CONFLICT OF INTEREST

The author declared no potential conflicts of interest with respect to the research, authorship, and/or publication of this article.

## ETHICS

There are no ethical issues with the publication of this manuscript.

## STATEMENT ON THE USE OF ARTIFICIAL INTELLIGENCE

Artificial intelligence was not used in the preparation of the article.

## REFERENCES

[1] Hussein EQ, Azziz HN, Rashid FL. Aerodynamic study of slotted flap for NACA 24012 airfoil by dynamic mesh techniques and visualization flow. J Therm Eng 2021;7:230-239. [CrossRef]
[2] Mahmoud H. Stability of turbine blades, aircraft wings and their acoustic radiation. J Therm Eng 2015;1. [CrossRef]
[3] Ayli E, Kocak E, Turkoğlu H. Numerical investigation of rod-airfoil configuration aeroacoustic characteristics using Ffowcs-Williams-Hawkings equations. J Therm Eng 2021;7:58-70. [CrossRef]
[4] Alpman E. Aerodynamic performance of small-scale horizontal axis wind turbines under two different extreme wind conditions. J Therm Eng 2015;1:420-432. [CrossRef]
[5] Maheri A. Simulation of wind turbines utilising smart blades. J Therm Eng 2016;2:557-565. [CrossRef]
[6] Boumehani A, Noura B, Kerfah R, Khelladi S, Dobrev I. Numerical investigation of the blade profile effect on the aerodynamic performance of a vertical-axis wind turbine Darrieus H-rotor. J Therm Eng 2020;6:388-396. [CrossRef]
[7] Şumnu A, Güzelbey İH. The effects of different wing configurations on missile aerodynamics. J Therm Eng 2023;9:1260-1271. [CrossRef]
[8] Arunvinthan S, Raatan VS, Nadaraja Pillai S, Pasha AA, Rahman MM, Juhany KA. Aerodynamic characteristics of shark scale-based vortex generators upon symmetrical airfoil. Energies (Basel) 2021;14:71808. [CrossRef]
[9] Domel AG, Saadat M, Weaver JC, Haj-Hariri H, Bertoldi K, Lauder GV. Shark skin-inspired designs that improve aerodynamic performance. J R Soc Interface 2018;15:139. [CrossRef]
[10] Lang AW, Hidalgo P. Cavity flow characterization of the bristled shark skin microgeometry. Bioinspir Biomim 2008;3:046005. [CrossRef]
[11] Lang AW, Motta P, Hidalgo P, Westcott M. Bristled shark skin: A microgeometry for boundary layer control? Bioinspir Biomim 2008;3:046005. [CrossRef]
[12] Santos LM, Lang A, Wahidi R, Bonacci A, Gautam S, Parsons J. The effect of shortfin mako shark skin at the reattachment of a separated turbulent boundary layer. Bioinspir Biomim 2024;19:5. [CrossRef]
[13] Natarajan E, Freitas LI, Rui Chang G, Abdulaziz Majeed Al-Talib A, Hassan CS, Ramesh S. The hydrodynamic behaviour of biologically inspired bristled shark skin vortex generator in submarine. Mater Today Proc 2021;46:3945-3950. [CrossRef]
[14] Pu X, Li GJ, Liu YH. Progress and perspective of studies on biomimetic shark skin drag reduction. ChemBioEng Rev 2016;3:26-40. [CrossRef]
[15] Han X, Zhang D. Study on the micro-replication of shark skin. Sci China Ser E: Technol Sci 2008;51:890-896. [CrossRef]
[16] Zhao DY, Huang ZP, Wang MJ, Wang T, Jin Y. Vacuum casting replication of micro-riblets on shark skin for drag-reducing applications. J Mater Process Technol 2012;212:198-202. [CrossRef]
[17] Walsh M, Lindemann A. Optimization and application of riblets for turbulent drag reduction. In: 22nd Aerospace Sciences Meeting. Reston, Virginia: American Institute of Aeronautics and Astronautics; 1984. [CrossRef]
[18] Schumacher JF, Favier A, Pinelli A, Piomelli U. Engineered antifouling microtopographies—effect of feature size, geometry, and roughness on settlement of zoospores of the green alga Ulva. Biofouling 2007;23:55-62. [CrossRef]
[19] Bixler GD, Bhushan B. Shark skin inspired low-drag microstructured surfaces in closed channel flow. J Colloid Interface Sci 2013;393:384-396. [CrossRef]
[20] Wen L, Weaver JC, Lauder GV. Biomimetic shark skin: Design, fabrication and hydrodynamic function. J Exp Biol 2014;217:1656-1666. [CrossRef]
[21] Fish FE. Influence of hydrodynamic design and propulsive mode on mammalian swimming energetics. Aust J Zool 1994;42:1-16. [CrossRef]

[22] Google Patent. Scalloped wing leading edge. Jun. 2000. Available at: https://patents.google.com/patent/US6431498B1/en Accessed Sep 04, 2025.
[23] Miklosovic DS, Murray MM, Howle LE, Fish FE. Leading-edge tubercles delay stall on humpback whale (Megaptera novaeangliae) flippers. Phys Fluids 2004;16:L39-L42. [CrossRef]
[24] Custodio D, Henoch CW, Johari H. Aerodynamic characteristics of finite span wings with leading-edge protuberances. AIAA J 2015;53:1878-1893. [CrossRef]
[25] Zhang MM, Wang GF, Xu JZ. Aerodynamic control of low-Reynolds-number airfoil with leading-edge protuberances. J AIAA J 2013;51:1960-1971. [CrossRef]
[26] Yoon HS, Hung PA, Jung JH, Kim MC. Effect of the wavy leading edge on hydrodynamic characteristics for flow around low aspect ratio wing. Comput Fluids 2011;49:276-289. [CrossRef]
[27] Kim MJ, Yoon HS, Jung JH, Chun HH, Park DW. Hydrodynamic characteristics for flow around wavy wings with different wave lengths. Int J Nav Arch Ocean Eng 2012;4:447-459. [CrossRef]
[28] Arunvinthan S, Gouri P, Divysha S, Devadharshini RK, Nithya Sree RN. Effect of trough incidence angle on the aerodynamic characteristics of a biomimetic leading-edge protuberanced (LEP) wing at various turbulence intensities. Biomimetics 2024;9:354. [CrossRef]
[29] Hansen KL, Kelso RM, Dally BB. Performance variations of leading-edge tubercles for distinct airfoil profiles. AIAA J 2011;49:185-194. [CrossRef]
[30] Analysis of the streamwise vortices generated between leading edge tubercles. Available at: https://www.researchgate.net/publication/258246709_Analysis_of_the_Streamwise_Vortices_Generated_Between_Leading_Edge_Tubercles Accessed on Nov 25, 2024.
[31] Flows in films and over flippers.. Available at: https://www.researchgate.net/publication/253904188_Flows_in_films_and_over_flippers Accessed on Nov 25, 2024
[32] Arunvinthan S, Nadaraja Pillai S, Cao S. Aerodynamic characteristics of variously modified leading-edge protuberanced (LEP) wind turbine blades under various turbulent intensities. J Wind Eng Ind Aerodyn 2020;202:104188. [CrossRef]
[33] Anderson JA. Fundamentals of Aerodynamics. Michigan: McGraw-Hill; 2001.
[34] Li Q, Kamada Y, Maeda T, Murata J, Nishida Y. Effect of turbulent inflows on airfoil performance for a horizontal axis wind turbine at low reynolds numbers (part I: Static pressure measurement). Energy 2016;111:701-712. [CrossRef]
[35] Arunvinthan S, Nadaraja Pillai S. Aerodynamic characteristics of unsymmetrical aerofoil at various turbulence intensities. Chin J Aeronaut 2019;32:2395-2407. [CrossRef]
[36] Barlow JB, Rae WH, Pope A. Low-speed Wind Tunnel Design. New York: John Wiley Sons; 1999.
[37] Skillen A, Revell A, Favier J, Pinelli A, Piomelli U. Investigation of wing stall delay effect due to an undulating leading edge: An LES study. In: 22nd Aerospace Sciences Meeting. Reston, Virginia: American Institute of Aeronautics and Astronautics; 2013. [CrossRef]